



HAL
open science

Strong intrusions of the Northern Mediterranean Current on the eastern Gulf of Lion: insights from in-situ observations and high resolution numerical modelling

Nicolas Barrier, Anne Petrenko, Yann Ourmieres

► **To cite this version:**

Nicolas Barrier, Anne Petrenko, Yann Ourmieres. Strong intrusions of the Northern Mediterranean Current on the eastern Gulf of Lion: insights from in-situ observations and high resolution numerical modelling. *Ocean Dynamics*, 2016, 66 (3), pp.313-327. 10.1007/s10236-016-0921-7 . hal-01436127

HAL Id: hal-01436127

<https://amu.hal.science/hal-01436127>

Submitted on 16 Jan 2017

HAL is a multi-disciplinary open access archive for the deposit and dissemination of scientific research documents, whether they are published or not. The documents may come from teaching and research institutions in France or abroad, or from public or private research centers.

L'archive ouverte pluridisciplinaire **HAL**, est destinée au dépôt et à la diffusion de documents scientifiques de niveau recherche, publiés ou non, émanant des établissements d'enseignement et de recherche français ou étrangers, des laboratoires publics ou privés.

**Strong intrusions of the Northern Mediterranean
Current on the eastern Gulf of Lion: insights from
in-situ observations and high resolution numerical
modelling**

Nicolas Barrier · Anne A. Petrenko ·

Yann Ourmières

Received: date / Accepted: date

Nicolas Barrier

Aix-Marseille Université, Université de Toulon, CNRS/INSU, IRD, MIO, UM 110, 13288
Marseille, France

Tel.: +33 4 86 09 06 12

E-mail: nicolas.barrier@univ-amu.fr

Anne A. Petrenko

Aix-Marseille Université, Université de Toulon, CNRS/INSU, IRD, MIO, UM 110, 13288
Marseille, France

Yann Ourmières

Université de Toulon, CNRS/INSU, IRD, MIO, UM 110, 83957 La Garde, Aix-Marseille
Université, CNRS/INSU, IRD, MIO, UM 110, 13288 Marseille,

Abstract The Northern Mediterranean Current is the return branch of the cyclonic circulation of the northwestern Mediterranean Sea. Because of geostrophic constraints, this warm and oligotrophic current is forced to flow westward along the continental slope of the Gulf of Lion. But, occasionally, it can penetrate on the shelf and strongly impacts the local biogeochemistry and in turn the primary production. By combining in-situ observations and high-resolution modelling, it is shown that intrusions on the eastern part of the gulf are mainly forced by easterly or northwesterly wind events, through physical mechanisms that are very different in nature.

Easterlies induce a piling of water along the Gulf of Lion coast that drives, through geostrophy, an alongshore shelf-intruding current. This intrusive current occurs independently of the stratification and is concomitant with the wind forcing. On the other hand, intrusions due to northwesterlies only occur during stratified conditions and are related to the development of upwellings along the Var coast. When the upwelling develops, a northwestward alongshore pressure force balances the Coriolis force associated with the onshore flow at depth. When the winds drop, the upwelling relaxes and the onshore flow weakens. Consequently, the Coriolis force no longer counterbalances the pressure force that ultimately dominates the momentum balance, causing the displacement of the Northern Current on the Gulf of Lion shelf approximately one day after the wind relaxation. This time lag between the northwesterlies's decrease and the intrusions permits to anticipate possible changes in the biogeochemistry of the Gulf of Lion.

Keywords Northern Current · Gulf of Lion · Intrusions · Julio · Upwelling · Cross-shelf exchanges · Wind-setup · Easterlies · Mistral · Tramontane · Northwesterlies

1 Introduction

Coastal areas are a key environment for the marine ecosystem, since they receive large amounts of nutrients through river outflows that in turn favour phytoplankton activity (Cruzado and Velasquez, 1990). They also play a significant role in the global biogeochemical cycles of carbon, nitrogen and phosphorus (Mantoura et al, 1991; Liu et al, 2000). But coastal areas are also subjected to high demographic pressure and consequently to great risks of pollution. In this context, a better understanding of the coastal circulation is critical since it controls the dispersion of anthropogenic and river-discharged pollutants (Huthnance, 1995), but also the advection of nutrients and larvae (Largier, 2003). This is especially true for the Gulf of Lion, which is a wide and shallow continental shelf in the northwestern Mediterranean Sea (Fig. 1), featuring a heavily urbanised shoreline.

Several forcings influence the coastal circulation in the Gulf of Lion. The Mistral and the Tramontane (hereafter referred to as northwesterlies) are cold and dry continental gusty winds that occur anytime in the year. They are highly constrained by the orography (Rhône river valley for the Mistral, Pyrenees and Massif Central for the Tramontane) and may therefore be associated with strong wind curls when they reach the gulf. In winter, through cooling

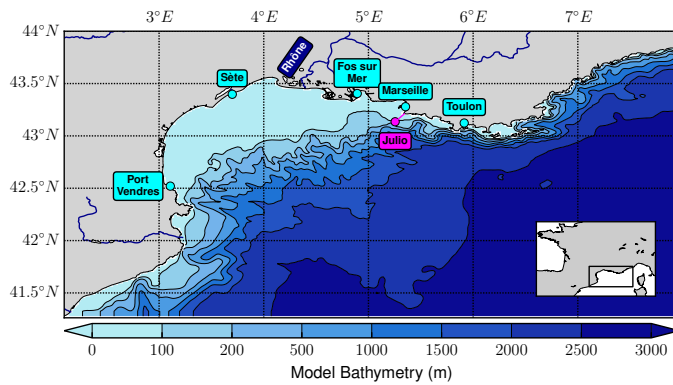


Fig. 1 Bathymetry of the Glazur64 configuration. The locations of the Julio mooring and section are indicated by a magenta point and a magenta line, respectively.

1 and evaporation, they may trigger dense water formation and cascading on the
 2 continental shelf (Ulses et al, 2008). While, in summer, they are associated with
 3 the development of upwellings (Millot, 1979). East-southeast winds (hereafter
 4 referred to as easterlies) carry clouds and rain over the Gulf of Lion and are
 5 associated with downwellings. They are less frequent than northwesterlies and
 6 are especially strong from autumn to spring (Millot, 1990). In addition to wind
 7 forcing, the Gulf of Lion is subjected to the freshwater inputs of the Rhône
 8 River. Its plume can extend over large areas when a strong volume discharge
 9 is combined with a shallow thermocline (Fraysse et al, 2014). The associated
 10 changes in the density field can impact the shelf circulation (Estournel et al,
 11 2001; Refray et al, 2004; André et al, 2005).

12 The coastal circulation in the Gulf of Lion is also strongly influenced by the
 13 large-scale ocean circulation of the Mediterranean. The Northern Current, also
 14 known as the “Liguro-Provençal Current”, is the northern branch of the cy-
 15 clonic gyre circulation of the northwestern Mediterranean Sea (Millot, 1999). It

1 originates before the Ligurian Sea from the merging of the Western and East-
2 ern Corsican Currents (Astraldi et al, 1990). This baroclinic current is, at first
3 order, in geostrophic balance and flows westward along the continental shelf.
4 During winter and certain upwelling conditions, the Northern Current sepa-
5 rates the fresh and nutrient-rich coastal waters from the salty and oligotrophic
6 offshore waters. But, as evidenced in observations and numerical modelling,
7 the Northern Current occasionally penetrates over the Gulf of Lion, causing
8 drastic changes in the biogeochemistry and in turn in the primary production
9 on the shelf (Ross et al, *in revision*).

10 Intrusions of a slope current on an adjacent shelf have already been ev-
11 idenced elsewhere in the world ocean, such as the surface intrusions of the
12 Gulf Stream (Oey et al, 1987; Gawarkiewicz et al, 1992) and of the Kuroshio
13 (Chen et al, 1996; Tang et al, 1999; Wu et al, 2005; Caruso et al, 2006).
14 Oey et al (1987) and Chen et al (1996) suggest that these intrusions are likely
15 forced by wind-induced onshore Ekman transport. Wu et al (2005) and Caruso
16 et al (2006) suggest that they are forced by strong wind-stress curls. Other
17 causes are also proposed, such as the meanderings of the main current (Oey
18 et al, 1987) or the abrupt changes in bottom topography (Chen et al, 1996).
19 The Gulf-Stream and the Kurushio currents are poleward currents that are
20 strongly influenced by the β -effect, contrary to the Northern Current that is
21 more zonally oriented. Other intrusions, more similar to those occurring on
22 the Gulf of Lion, have been evidenced on the northwestern shelf of the Black
23 Sea (Oguz and Besiktepe, 1999; Korotaev et al, 2003) or on the Papua Gulf

1 in New Guinea (Wolanski et al, 1995). However, the physical mechanisms of
2 these intrusions have not been investigated yet.

3 Intrusions of the Northern Current on the eastern part of the Gulf of Lion
4 have been investigated by Gatti et al (2006) and Gatti (2008), using a combi-
5 nation of in-situ observations and numerical modelling. The authors suggest
6 that some intrusions are forced by easterlies, through either Ekman transport
7 or a shoreward displacement of the Northern Current. They also propose that
8 northwesterlies may favour intrusions through the associated positive wind-
9 stress curl. This curl would provide a source of vorticity to the Northern
10 Current that may drive intrusions. She also suggests that intrusions on the
11 eastern part of the Gulf of Lion are also likely to occur after the relaxation
12 of upwelling-favourable winds, as shown by Millot and Wald (1980). Using
13 analytical model and numerical simulations, Echevin et al (2003) assessed the
14 interaction between a coastal current, represented as a baroclinic Kelvin wave,
15 and a shelf break. They suggest that Ekman transport associated with south-
16 easterlies induce a downwelling, which in turn generates a westward coastal
17 current that transports Northern Current waters onto the shelf.

18 Therefore, although the intrusions of the Northern Current on the eastern
19 part of the Gulf of Lion have been shown to be wind-driven, the associated
20 physical mechanisms remain unclear. Furthermore, the potential influence of
21 the ocean stratification is also not well understood. For instance, Millot and
22 Wald (1980) suggest that intrusions of the Northern Current occur when the

1 ocean is stratified, while Petrenko (2003) has shown that intrusions may be
2 observed independently of stratification.

3 The aim of the present study is to address these uncertainties and therefore
4 to gain more understanding on the physical mechanisms behind the intrusions
5 of slope current on continental shelves. Using a combination of ADCP current
6 observations, tide-gauge data and regional high resolution numerical mod-
7 elling, the physical mechanisms that link the wind forcings and the intrusions
8 on the eastern part of the gulf are investigated for the 2012-2013 period. The
9 paper is organised as follows. In section 2, the observations and numerical
10 model are described. In section 3, the methodology used in the detection of
11 simulated and observed intrusions is presented. Section 4 is dedicated to the
12 analysis of the physical mechanisms that drive the intrusions. Conclusions and
13 discussions are provided in section 5.

14 **2 Data description**

15 2.1 Julio mooring

16 Gatti (2008) has suggested that the Julio¹ site, located on the 100 m isobath
17 at 5.255°E-43.135°N (magenta point in Fig. 1), is a judicious location for the
18 observation of intrusions occurring on the eastern side of the Gulf of Lion. As
19 such, it has been proposed as a site in the framework of the MOOSE² observing
20 system (<http://www.moose-network.fr/>). A bottom-moored ADCP (RDI

¹ Judicious Location for Intrusion Observation

² Mediterranean Ocean Observing System for the Environment

1 Ocean Sentinel, 300 kHz) at the Julio site is exploited from 2012-02-12 to
 2 2012-10-23 and from 2013-09-26 to 2013-12-31. It provides measurements of
 3 the horizontal currents every 30 minutes and every 4 m depth between 15 m
 4 and 92 m.

5 2.2 Sonel tide-gauge data

6 Daily tide-gauge observations at Fos sur Mer, Sète and Port Vendres (see
 7 locations on Fig. 1) are downloaded from the Sonel website (Sonel stands
 8 for “Système d’Observation du Niveau des Eaux Littorales”; website: <http://www.sonel.org/>). The inverted barometer effect η^{ibc} is computed following
 9 Ponte (2006) by:
 10

$$\eta^{ibc} = -\frac{p_a - \bar{p}_a}{\rho_0 g}$$

11 and is subtracted from the raw daily timeseries. p_a is the atmospheric sea-
 12 level pressure and \bar{p}_a its long-term mean (computed on the 1979-2014 period),
 13 ρ_0 the reference density of water (here, 1000 kg.m^{-3}) and g the gravity. The
 14 sea-level pressure used here is issued from the ERA-Interim reanalysis of the
 15 European Centre for Medium-Range Weather Forecasts (Dee et al, 2011).

16 2.3 High-resolution numerical modelling

17 The physical mechanisms that drive the intrusions of the Northern Current on
 18 the eastern part of the Gulf of Lion are investigated using the high resolution
 19 model simulations of Guihou et al (2013), which are derived from the Glazur64

1 configuration of Ourmières et al (2011). Glazur64 is based on the “Nucleus for
2 European Modelling of the Ocean” modelling framework (NEMO, Madec,
3 2008) and is implemented on a $1/64^\circ$ regular grid with 130 vertical z-levels,
4 spacing from 1 m near the surface to 30 m near the bottom. The ocean bound-
5 ary conditions at the eastern and southern parts of the domain use radiative
6 type conditions (Cailleau et al, 2008), with boundary data prepared from the
7 basin-scale PSY2V4R1 operational configuration provided by MERCATOR-
8 OCEAN (<http://www.mercator-ocean.fr>). The damping coefficients for the
9 inflows and the outflows are 1 and 10 days, respectively.

10 Surface boundary conditions are provided by the Météo France operational
11 regional model Aladin. This atmospheric model features data assimilation and
12 state-of-the-art atmospheric physics (Fischer et al, 2005). It has a horizontal
13 resolution of around $1/10^\circ$ (9.5 km) and forcings are provided every 3h. Such
14 spatio-temporal resolution has shown to well reproduce specific wind systems,
15 diurnal cycles and sea breeze, hence leading to a valuable improvement of the
16 mesoscale circulation simulated by the ocean model (Schaeffer et al, 2011).
17 The reader interested in the details of the Glazur64 configuration are referred
18 to Guihou et al (2013).

19 2.4 Comparison of Glazur64 with the Julio mooring

20 The time-averaged simulated velocity profiles at the Julio site are compared
21 with the observed ones. The meridional component is fairly well captured by
22 the model simulation, both in term of magnitude and vertical structure (Fig. 2,

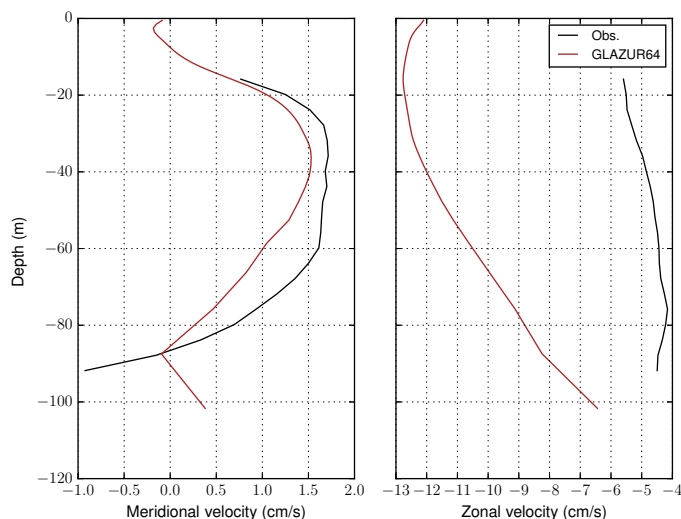


Fig. 2 Time-averaged of the observed (black) and simulated (red) velocity profiles at the Julio site, computed over the overlapping time period between the observations and model simulation (from February to the end of October 2012, and from October to December 2013).

1 left panel). However, Glazur64 strongly overestimates the zonal component of
 2 the current at the Julio site (Fig. 2, right panel): the simulated zonal velocity
 3 is indeed twice as large as the observed one and shows a large weakening
 4 at depths, while the observed profile is more homogeneous. This discrepancy
 5 is presumably due to a misposition of the simulated Northern Current, which
 6 may be too close to the coast hence encroaching on the Julio location. However,
 7 this model bias is not critical for the comparison of observed and simulated
 8 intrusions. Indeed, more relevant indexes to detect the presence of intrusions
 9 will be presented in the following section

3 Detection of Northern Current's intrusions

The intrusions of the Northern Current on the eastern part of the Gulf of Lion have been detected using the Julio ADCP mooring observations as follows. First, the current component that flows perpendicular to the Julio section (magenta line at angle $\theta = 49.4^\circ$ from north in Fig. 1) has been computed using the measured zonal and meridional velocities:

$$U_{jul} = V \cos \theta - U \sin \theta$$

with V and U the meridional and zonal velocities at the Julio mooring. By convention, U_{jul} is counted positive for a northwestward flowing current. Then, U_{jul} has been vertically averaged, hence leading to a half-hourly time-series, on which daily averaging has been performed. Finally, the resulting daily time-series has been standardised: the temporal mean, computed over the overlapping time-period between the observations and model simulation, has been removed and the resulting anomalies have been divided by their standard deviation. The resulting standardized index, which will be referred to as the “observed” Julio index, is shown in Fig. 3 (black line). In the following, we will consider that intrusions occur, in the in-situ data, when the observed Julio index is greater than 1, i.e. when the depth-averaged across-section velocity exceeds its mean by 1 standard deviation.

The same methodology is applied on the Glazur64 model simulation at the grid point the closest to Julio. As expected from figure 2, the temporal mean of the simulated U_{jul} velocity is overestimated when compared with

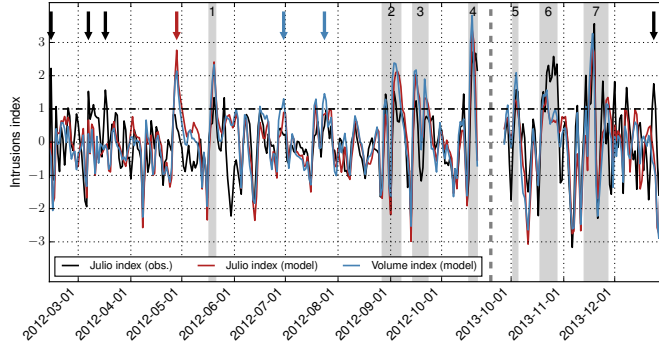


Fig. 3 Observed (black line) and simulated (red and blue lines) standardised intrusion indexes. Only the overlapping time period between the observations and model simulation (from February to the end of October 2012, and from October to December 2013) is shown. Black arrows indicate intrusion events that are observed but not simulated, the red arrow indicates the simulated intrusion event which is not observed and blue arrows highlight simulated intrusions that are captured by the volume index but not by the Julio one. The vertical dotted line separates the two time series. The horizontal dotted line corresponds to the detection threshold. The grey shadings highlight the intrusion events that are investigated in section 4.

1 the observed one (8.4 cm.s^{-1} and 4.3 cm.s^{-1} , respectively). However, their
 2 standard deviations are very similar (10.3 cm.s^{-1} and 9.1 cm.s^{-1} for the
 3 observations and model simulation, respectively). The simulated standardized
 4 Julio index (red line in Fig. 3) shows a correlation of 0.59 with the observed
 5 index. This correlation is significant at the 95% level of confidence, according to
 6 a Student t-test in which the number of degrees of freedom has been corrected
 7 from the 1-day lag autocorrelation of both time series (Bretherton et al, 1999).
 8 As shown in Fig. 3, there is a good agreement between the occurrence of the
 9 simulated and observed intrusions, in spite of the overestimated zonal velocity

1 simulated at Julio. The model simulation can therefore be considered as robust
2 enough to investigate the physical mechanisms that are responsible for the
3 intrusions.

4 Nevertheless, there are some examples when the two indexes are out of
5 phase. For example, five intrusion events are observed but are not reproduced
6 in Glazur64 (black arrows on Fig. 3). On 2012-02-14, the observed index has
7 a value of 2.2, while the simulated one has a value of 0.0. On 2012-03-07 the
8 observed index is 1.5 and the simulated one is 0.7, while on 2012-03-17, the ob-
9 served index is 1.56 and the simulated one is -0.1. On 2013-12-24, the observed
10 Julio index reaches 1.7 and remains above 1 the next day, while the simulated
11 index has a value of -0.4. On 2013-12-29, the observed Julio index reaches 1.6
12 and increases up to 2.1 the next day, while the simulated Julio index has a
13 value of -1.5. Conversely, one strong intrusion event is simulated on 2012-04-
14 27 by the model but is not observed (red arrow on Fig. 3). At this time, the
15 simulated Julio index reaches 2 and remains above 1 the following 4 days, with
16 a maximum value of 2.8 on 2012-04-28. The observed index also shows an in-
17 crease but remains below the detection threshold. These discrepancies might
18 be due to an underestimation by the numerical model of the higher levels of
19 instability of the Northern Current during winter, or to a misrepresentation
20 of wind forcings by the Aladin model. However, the lack of data observations
21 prevents us from providing robust conclusions. Therefore, we decided to con-
22 centrate our efforts on the understanding of the forcing mechanisms of the
23 intrusions which are both observed and simulated.

1 In order to assess the robustness of the Julio index in the detection of
2 intrusive events, another methodology is added in Glazur64. Daily volume
3 transport across the Julio section is computed by using the “Physical Analy-
4 sis of the Gridded Ocean” (PAGO) suite of programs (Deshayes et al, 2014)³.
5 PAGO permits the computation of transport indexes along predefined sections
6 with limited interpolation by connecting two section endpoints as a continu-
7 ous sequence of grid faces following a great circle pathway. Current velocities
8 along the section do not undergo any interpolation, hence allowing a better
9 precision on the volume transport calculation. The calculated volume trans-
10 port is standardised in the same way as the Julio index. This simulated volume
11 index (blue line in Fig. 3) is highly correlated with the simulated Julio index
12 (correlation of 0.92, significant at the 95% level of confidence), and both simu-
13 lated indexes detect the same intrusion events. Therefore, the simulated Julio
14 index provides a good indicator of the simulated volume transport between
15 the coast, and the comparison between the in-situ and simulated Julio indexes
16 provide a good indicator for concomitant intrusion events.

17 However, we can mention the rare cases of intrusions that are confined very
18 close to the coast. These intrusions are characterized by a simulated volume
19 index that is above 1 and by Julio indexes (observed and simulated) that are
20 less than 1 (blue arrows of Fig. 3). This is for instance the case for the intrusion
21 event that starts on 2012-07-23, during which the simulated volume transport

³ See also <http://www.whoi.edu/science/PO/pago/>

Table 1 List of intrusions that are investigated in section 4. NW stands for northwesterlies and E for easterlies.

Number	Start Date	End Date	Wind Forcing
I1	2012-05-18	2012-05-21	NW+E
I2	2012-08-28	2012-09-07	NW
I3	2012-09-15	2012-09-23	NW
I4	2012-10-18	2012-10-22	NW+E
I5	2013-10-03	2013-10-05	E
I6	2013-10-19	2013-10-28	E
I7	2013-11-14	2013-11-27	NW+E

1 index is above 1 for 3 days, while the simulated Julio index reaches a maximum
 2 of 0.9, hence below the detection threshold.

3 **4 Physical mechanisms of the intrusions**

4 In this section, the physical mechanisms associated with the intrusions are
 5 investigated. We have focused our attention only on strong intrusion events
 6 (grey shadings in Fig. 3, see also Table 1), during which all three intrusion
 7 indexes are larger than 1 at least one day, hence corresponding to variations
 8 superior to their standard deviations. Moreover, we chose to merge intrusions
 9 when only 1 or 2 days separate them. It is the case of intrusions I2 and I3
 10 that both include two intrusions when one looks at the details of Fig. 3.
 11 The physical mechanisms associated with these intrusion events are described
 12 in the following.

1 4.1 Intrusions due to easterlies

2 Intrusions I5 and I6 occur during easterly wind conditions. As discussed in
3 the introduction, easterlies carry rain and clouds over the Gulf of Lion. In
4 the model simulation, intrusions due to easterlies are associated with a very
5 strong increase in sea-surface height over the Gulf of Lion, as shown for in-
6 stance in Fig. 4 for intrusion I6. Such an increase is also evidenced in the Sonel
7 tide-gauge observations: sea-surface height at Fos sur Mer and Sète shows an
8 increase of approximately 20 cm during intrusions 5 and 6 (Fig. 5). This in-
9 crease is in agreement with the wind setup mechanism proposed by Csanady
10 (1982), which characterizes a balance between the wind-stress and the hor-
11 izontal pressure gradients associated with the sea-level slope. The increase
12 in across-shore pressure gradient induces a geostrophic westward alongshore
13 current until 4°E and southwestward west of 4°E.

14 As discussed in Fraysse et al (2014), easterlies are also associated with
15 downwelling conditions along the coast. In the model simulation, downwelling
16 indeed occurs, as confirmed by the presence at 20 m depth of diluted freshwater
17 ($S \approx 37.2$) originating from the Rhône river (Fig. 6, panel c), consistently with
18 Fraysse et al (2014). This freshwater plume is then advected westward past 4°E
19 by the intruding current (Fig. 6, panels d and e). Furthermore, as discussed
20 by Echevin et al (2003), the downwelling of warm (in summer) and freshwater
21 may also contribute significantly to the westward coastal current.

22 Fig. 7 shows the smoothed, daily climatology of the simulated temperature
23 at Julio, which represents well what occurs in the region (data not shown). It is

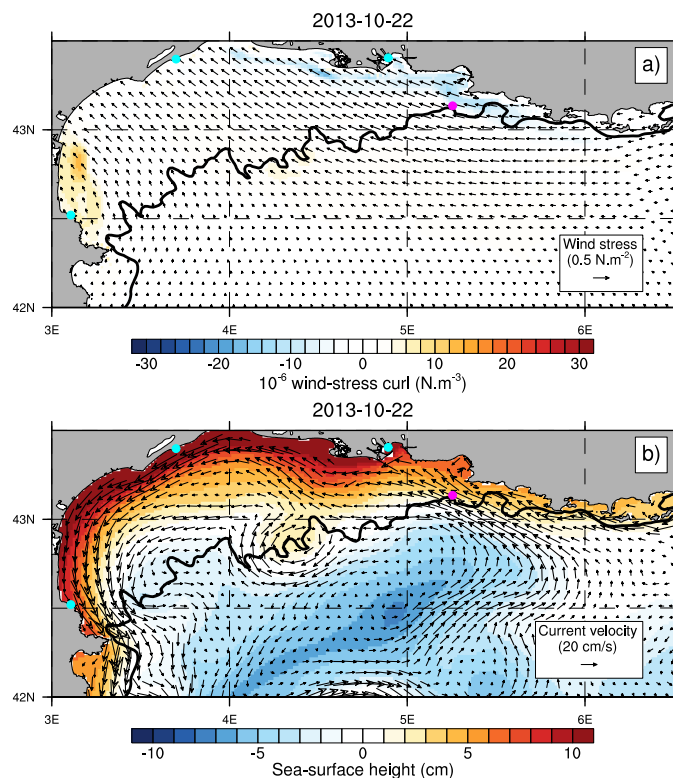


Fig. 4 Top panel: simulated wind-stress (arrows) and wind-stress curl (color shadings) during intrusion I6. Bottom panel: simulated sea-surface height (color shadings) and 20 m current velocity (arrows) during intrusion I6. The locations of the Snel tide-gauge stations and of the Julio mooring are shown in cyan and magenta, respectively. The 200-m isobath is shown with a bold black line.

1 constructed as follows. For each water depth, the daily climatology is computed
 2 over the 2012-2013 period of the simulation and the FFT coefficients of this
 3 climatology are computed. Then, all the harmonics but the annual and semi-
 4 annual ones are artificially set to 0. The smoothed daily climatology is finally
 5 reconstructed by computing the inverse FFT on these new FFT coefficients. As
 6 can be inferred from Fig. 7, intrusions I5 and I6 occur in November when the

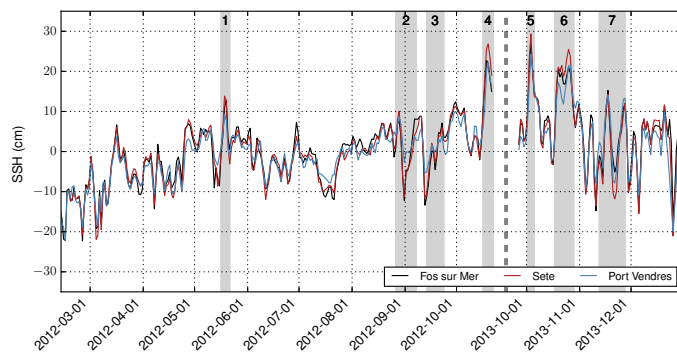


Fig. 5 Daily sea-surface height anomalies from the Sonel dataset corrected from the inverted barometer effect (see section 2.2 for details). Anomalies have been computed by removing the 2012-2013 mean. The vertical dotted line separates the two time series. The grey shadings highlight the intrusion events that are investigated in section 4.

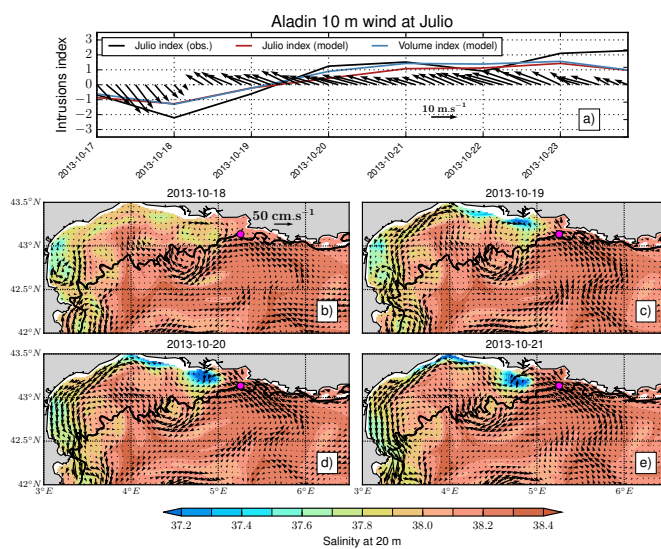


Fig. 6 Top panel: Aladin wind at Julio (arrows) and intrusion indexes (lines). Bottom panels: simulated salinity (color shadings) and ocean currents (arrows) at 20 m during intrusion I6. The 200-m isobath is shown with a bold black line.

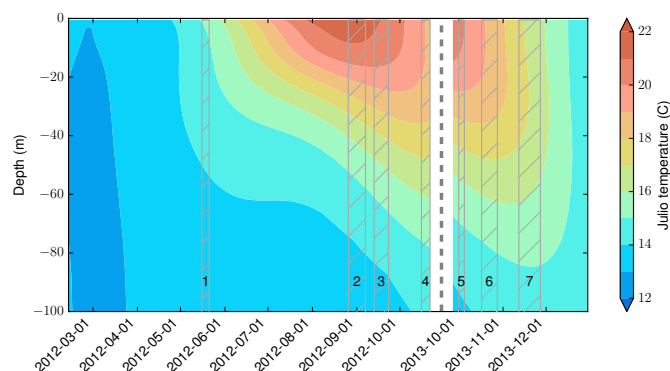


Fig. 7 Hövmoller diagram of the smoothed daily climatology of the simulated temperature at the Julio location (annual and semi-annual harmonics retained, see text for details). The vertical dotted line separates the two time series. The grey hatchings indicate the intrusion events that are investigated in section 4.

1 ocean is stratified. However, intrusions induced by easterlies may also occur
 2 during unstratified conditions, as for instance between 2012-04-27 and 2012-
 3 05-01. As shown in Fig. 3, the simulated Julio and volume indexes are greater
 4 than 2, hence suggesting that a very strong intrusion occurs in the model
 5 simulation at this time. This April intrusion shows the same characteristics as
 6 intrusions I5 and I6. We can then conclude that given the barotropic nature
 7 of the mechanism described above, intrusions in response to easterlies occur
 8 independently of the stratification.

9 4.2 Intrusions due to northwesterlies

10 Intrusions I2 and I3 are induced by strong northwesterly wind bursts on 2012-
 11 08-26 and 2012-08-31 for I2 (top panel of Fig. 8), 2012-09-13 and 2012-09-19
 12 for I3. These wind events are followed by intrusions of the Northern Current

1 that reach the Julio location one day after the wind relaxation, i.e. on 2012-
2 08-28 and 2012-09-02 for I2, on 2012-09-15 and 2012-09-21 for I3. Indeed,
3 one can observe negative indexes during I2 and I3 concomittant with blowing
4 northwesterlies, and positive indexes after their relaxation (top panel of Fig.
5 8).

6 Using satellite sea-surface temperature, Millot and Wald (1980) have shown
7 that such wind patterns are favourable to upwellings along the Gulf of Lion
8 coasts and that, when the wind relaxes, the frontal zone between the cold
9 upwelled waters and the warm waters originating from the Northern Current
10 tends to move northwestward and to penetrate over the shelf. As shown in
11 Fig. 8 for intrusion I2, this behaviour is reproduced by the Glazur64 model
12 simulation. When the wind blows, the ocean currents at 20 m beyond the 200
13 m isobath are southwestward, reflecting the ocean response to wind-stress via
14 Ekman transport (Fig. 8, panel b). Upwellings start developing along all linear
15 coasts and shows maximum vertical velocities on the shelf between Marseille
16 and Toulon, collocated with the strongly positive wind-stress curl (data not
17 shown). The upwelling reaches its maximum amplitude on 2012-09-01 (Fig. 8,
18 panel c), when the wind relaxes. The Northern Current reaches the Julio loca-
19 tion on 2012-09-02 (Fig. 8, panel d), hence one day after the wind relaxation.

20 The sea-surface height pattern associated with the intrusions induced by
21 northwesterlies (Fig. 9) is very different from the one associated with the in-
22 trusions driven by easterlies (Fig. 4). First, the sea-surface height on the Gulf
23 of Lion coast is not much impacted. This is further confirmed by the observa-

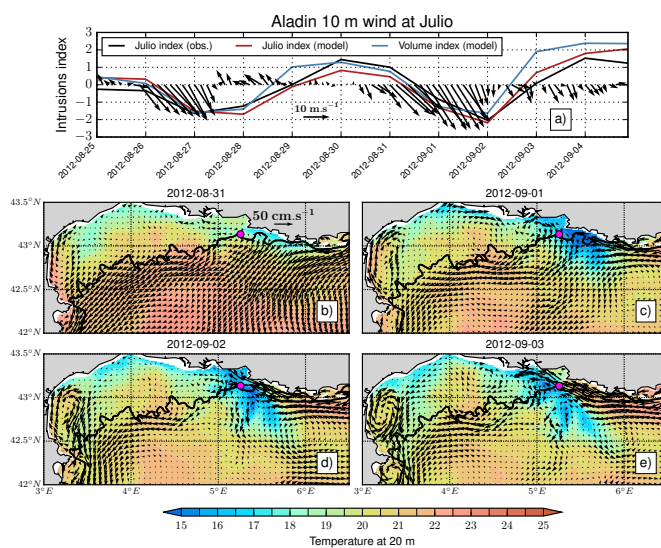


Fig. 8 Top panel: Aladin wind at Julio (arrows) and intrusion indexes (lines). Bottom panels: simulated temperature (color shadings) and ocean currents (black arrows) at 20 m during intrusion I2. The 200-m isobath is shown with a bold black line.

1 tions at the Sonel stations during intrusions I2 and I3, which show a decrease
 2 and negative anomalies rather than the increase and positive anomalies of the
 3 other intrusions (Fig. 5). Furthermore, one can observe that the sea-surface
 4 height pattern on 2012-09-03 (Fig. 9) shows negative values centred at ap-
 5 proximately 6°E , 42.5°N , which are tilted northwestward, and positive values
 6 on the shelf along the Var coast. The negative values near 6°E and 43°N are
 7 collocated and move with the cold temperature pattern of Fig. 8 (Fig. 8, pan-
 8 els c, d, e). This sea-surface height pattern is associated with positive zonal
 9 gradients near 5.25°E and with negative zonal gradients near 5°E . Interest-
 10 ingly, these gradients provide a good indicator of the pressure gradients at
 11 20 m (data not shown). The positive pressure gradients on the east induce a

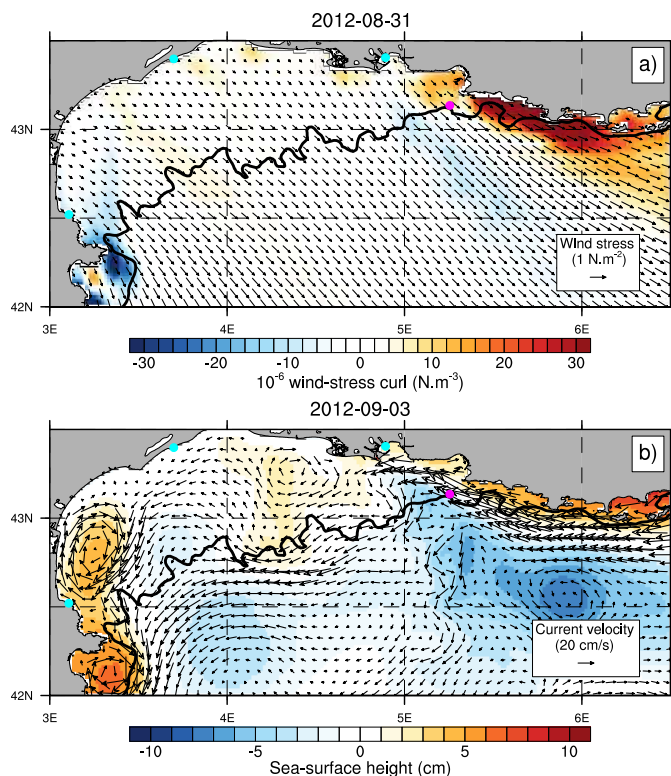


Fig. 9 Top panel: simulated wind-stress (arrows) and wind-stress curl (color shadings) during intrusion I2. Bottom panel: simulated sea-surface height (color shadings) and 20 m current velocity (arrows) during intrusion I2. The locations of the Soneil tide-gauge stations and of the Julio mooring are shown in cyan and magenta, respectively. The 200-m isobath is shown with a bold black line.

1 northwestward force that is likely to be responsible for the displacement of the
 2 Northern Current on the Gulf of Lion shelf.

3 This evolution of the Northern Current after northwesterly wind bursts can
 4 be related to what happens on the continental shelf off California, as described
 5 by Gan and Allen (2002). During northwesterly upwelling favourable winds,
 6 negative zonal pressure gradients develop west of the Cape Croisette (located

1 south of Marseille, at the north-eastern end of the Julio section, Fig. 1), bal-
2 ancing the nonlinear advective effects, while east of the cape, positive zonal
3 pressure gradients geostrophically balance the onshore flow at depth. When
4 the northwesterly winds drop, the upwelling relaxes and the Coriolis force no
5 longer counterbalances the westward pressure force that ultimately dominates
6 the momentum balance, hence accelerating the current westward. But west of
7 capes, the eastward pressure force is still balanced by the nonlinear advective
8 effects and hence does not contribute to accelerate the current eastward. The
9 net effect is therefore a westward flowing current.

10 Contrary to the easterlies, which may trigger intrusions any time of the
11 year, northwesterlies do not always yield intrusions. For example, in 2012-03-
12 05, the simulated wind-stress is very close to the one simulated on 2012-08-31
13 (compare Fig. 10 with Fig. 9). But this wind burst is not associated with an
14 upwelling nor with an intrusion on the following days (Fig. 10).. The tem-
15 perature pattern following the wind burst shows colder temperatures on the
16 western Gulf of Lion coasts and rather homogenous temperatures in the open
17 sea (figure not shown). Simulated daily temperature anomalies at Julio, com-
18 puted by removing the smoothed seasonal cycle shown in Fig. 7, show reduced
19 variance between December and April both at the surface and at 20 m depth
20 (data not shown). This tends to confirm the absence of upwellings during the
21 unstratified winter season. A similar behaviour has been evidenced on the
22 North Carolina shelf by Lentz (2001), who suggests that, during unstratified

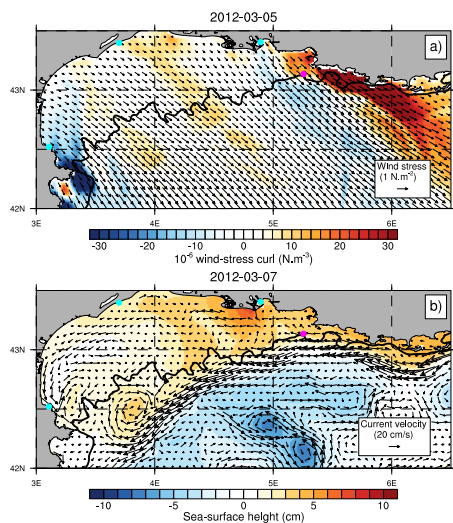


Fig. 10 Top panel: simulated wind-stress (arrows) and wind-stress curl (color shadings) on 2012-03-05. Bottom panel: simulated sea-surface height (color shadings) and 20 m current velocity (arrows) on 2012-03-07. The locations of the Sonel tide-gauge stations and of the Julio mooring are shown in cyan and magenta, respectively. The 200-m isobath is shown with a bold black line.

1 conditions, the wind-driven cross-shelf circulation is weaker because the Ek-
 2 man depth is greater than the water depth.

3 4.3 Combination of both wind patterns

4 Intrusions I1, I4 and I7 are due to a combination of northwesterlies and east-
 5 erlies. For I1, the intrusion is triggered by a strong northwesterly wind event
 6 on 2012-05-16. Following the mechanisms described in section 4.2, the current
 7 starts intruding on the shelf on 2012-05-18. This intrusion is then reinforced
 8 by strong easterlies that blow on 2012-05-19 and 2012-05-20, which induce a
 9 strong increase in sea-surface height on the western part of the Gulf of Lion

1 and accelerate the intrusive current as discussed in section 4.1. Similar pat-
2 terns occur for the other two intrusions. In short, intrusion I4 is triggered by
3 northwesterlies blowing on 2012-10-15 and is reinforced by easterlies blowing
4 between 2012-10-18 and 2012-10-20. Intrusion I7 is triggered by the northwest-
5 erlies of 2013-11-14 and reinforced by the easterlies blowing on 2013-11-17 and
6 2013-11-18.

7 **5 Discussion and conclusions**

8 In this paper, the physical mechanisms associated with the intrusions of the
9 Northern Current on the eastern side of the Gulf of Lion have been investigated
10 using a combination of in-situ observations (Julio ADCP mooring and Sonel
11 tide-gauge data) and high resolution numerical modelling. We have shown that
12 easterlies and northwesterlies are likely to favour such intrusions, but through
13 physical mechanisms that are very different in nature. Easterlies generate in-
14 trusions through a wind-setup mechanism and an increase in sea-surface height
15 along the coast, which induces a geostrophic alongshore northwestward coastal
16 current. Because of the barotropic nature of this mechanism, easterlies are
17 favourable to intrusions independently of the stratification and thus any time
18 of the year. On the other hand, intrusions in response to northwesterlies princi-
19 pally occur during stratified conditions and are associated with the relaxation
20 of the upwelling that occurs between Marseille and Toulon (Fig. 1). When the
21 upwelling develops, the Coriolis force associated with the onshore flow balances
22 a northwestward pressure gradient force. But when the winds drop and the

1 upwelling relaxes, the Coriolis force weakens and the pressure force dominates
2 the momentum balance. Consequently, the current is advected northwestward
3 and reaches the Julio location approximately one day after the wind relaxation.
4 This is very close to the mechanism that takes place in the upwelling system
5 off northern California, as discussed for instance in Gan and Allen (2002).

6 The difference in the physical mechanisms associated with these two wind
7 patterns may be evidenced using the Julio mooring observations and the Al-
8 adin wind fields by using lead-lag covariance analysis. 3-hourly wind-anomalies
9 are first computed by removing the 2012-2013 mean. The lead-lag covariances
10 between these wind-anomalies and the 3-hourly Julio index (obtained by aver-
11 aging the half-hourly across-section velocity and by standardising the result-
12 ing time-series) are then computed for each grid point. These covariance maps
13 measure how much the Julio index and the wind anomalies vary together as
14 a function of the time lag between the two series. They have the same units
15 as the wind-anomalies and the visual inspection of the covariance maps shows
16 that the strength of the covariance increases from 0-lag to 9 hours lag (wind
17 anomalies lead), at which point it shows a pattern similar to an easterly wind
18 pattern (Fig. 11, top panel). The covariance then decreases in the Gulf of Lion
19 until lag 39 hours, where it reaches a minimum. Then, the covariance increases
20 until lag 81 hours (approximately 3 days), when it reaches a secondary maxi-
21 mum of weaker amplitude than the first one, looking like a northwesterly-like
22 wind pattern (Fig. 11, bottom panel). This covariance analysis is consistent

1 with the results described in the above, namely a fast response of the Northern
2 Current intrusions to easterlies and a delayed response to northwesterlies.

3 A remaining question, however, is whether easterlies or northwesterlies are
4 necessary or sufficient conditions for intrusions of the Northern Current on
5 the eastern part of the Gulf of Lion. Fig. 12a shows the simulated wind-stress
6 at the Julio location and the orientation of strong wind events (defined as
7 periods when the wind-stress amplitude exceeds its mean by one standard-
8 deviation), while Fig.12b shows the simulated volume index over the entire
9 2012-2013 period. One can notice that, as discussed in section 4.1, strong
10 easterly wind events are always associated with a sharp increase in volume
11 transport across the Julio section, and can therefore be considered as sufficient
12 conditions for intrusions. However, as discussed in section 4.2, northwesterlies
13 are associated with intrusions mainly in summer, when the ocean is stratified
14 (cf. Fig 7). Hence northwesterlies are not sufficient conditions for intrusions.
15 But some intrusion events may also occur when the wind forcing is weak,
16 as for instance in November 2012. These events correspond to meanders of
17 the Northern Current encroaching on the shelf, which are presumably due to
18 instabilities of the Northern Current, as discussed in Gatti (2008). Therefore,
19 neither type of wind is a necessary condition, since intrusions can occur without
20 strong winds.

21 Nevertheless, the results of the present study are promising since they po-
22 tentially allow to anticipate cross-shore transports and potential intrusions on
23 the shelf of current-carried plankton or pollution. For instance, Berline et al

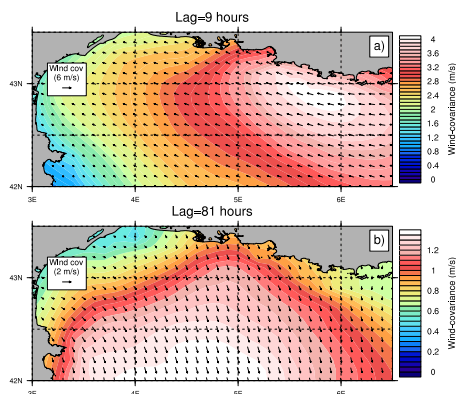


Fig. 11 Covariance at lag 9 hours (top panel) and 81 hours (bottom panel) between the 3-hourly standardised Julio index and the Aladin wind anomalies (wind anomalies lead). Note that the color and arrow scales are different between the two panels.

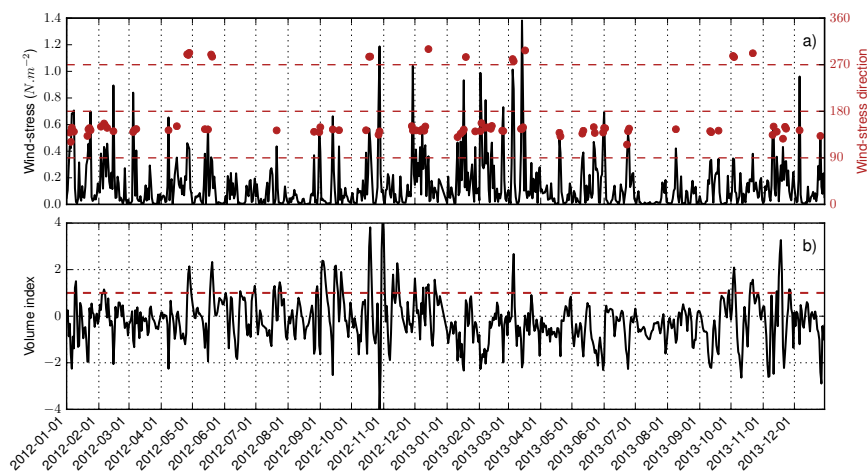


Fig. 12 Top panel: Wind-stress amplitude at the Julio location as simulated by the Glazur64 model. Red dots indicate the direction of strong wind events (defined as periods when the wind-stress amplitude exceeds the mean by one standard-deviation). Southerlies=0, Westerlies=90, Northerlies=180, Easterlies=270. Bottom panel: simulated volume index over the entire 2012-2013 period. The dashed line depicts the intrusion detection criteria.

1 (2013) suggest, using the Glazur64 model configuration and a Lagrangian par-
2 ticle tracking software, that jellyfishes are more abundant on the Ligurian
3 Sea coast when the Northern Current is close to the shore. Given the results
4 described in the present study, one can suggest that increased transport of jel-
5 lyfish on the Gulf of Lion coast may be anticipated in the case of northwesterly
6 winds under stratified conditions, since the intrusions occur one day after the
7 wind relaxes. However, for the intrusions associated with easterlies, since they
8 occur in phase with the wind forcing, the anticipation of jellyfish stranding
9 is likely to depend on the skill of the weather forecast to predict such wind
10 events. Improving our understanding of the physical processes controlling the
11 environmental conditions of coastal regions have significant socio-economical
12 implications, especially regarding fisheries and marine pollution.

13 **Acknowledgements** The authors thank Gilles Rougier and Denis Malengros for their
14 technical assistance with the Julio mooring. The Glazur64 simulations were performed us-
15 ing GENCI-IDRIS resources (Grant 2014011707). The analysis and plots of this paper were
16 performed with both Python and the NCAR Command Language (version 6.2.1, 2011, Boul-
17 der, Colorado, UCAR/NCAR/CISL/VETS, <http://dx.doi.org/10.5065/D6WD3XH5>). The
18 authors also acknowledge Julie Gatti, whose thesis strongly influenced this work.

19 **References**

20 André G, Garreau P, Garnier V, Fraunié P (2005) Modelled variability of
21 the sea surface circulation in the North-western Mediterranean Sea and
22 in the Gulf of Lions. *Ocean Dynamics* 55(3-4):294-308, DOI 10.1007/

1 s10236-005-0013-6

2 Astraldi M, Gasparini G, Manzella G, Hopkins T (1990) Temporal Variability
3 of Currents in the Eastern Ligurian Sea. *Journal of Geophysical Research-*
4 *Oceans* 95(C2):1515–1522, DOI 10.1029/JC095iC02p01515

5 Berline L, Zakardjian B, Molcard A, Ourmières Y, Guihou K (2013) Modeling
6 jellyfish *Pelagia noctiluca* transport and stranding in the Ligurian Sea. *Ma-*
7 *rine Pollution Bulletin* 70(12):90–99, DOI 10.1016/j.marpolbul.2013.02.016

8 Bretherton C, Widmann M, Dymnikov V, Wallace J, Blade I (1999) The ef-
9 fective number of spatial degrees of freedom of a time-varying field. *Jour-*
10 *nal of Climate* 12(7):1990–2009, DOI 10.1175/1520-0442(1999)012<1990:
11 TENOSD>2.0.CO;2

12 Cailleau S, Fedorenko V, Barnier B, Blayo E, Debreu L (2008) Comparison of
13 different numerical methods used to handle the open boundary of a regional
14 ocean circulation model of the Bay of Biscay. *Ocean Modelling* 25(12):1–16,
15 DOI 10.1016/j.ocemod.2008.05.009

16 Caruso MJ, Gawarkiewicz GG, Beardsley RC (2006) Interannual variability
17 of the Kuroshio intrusion in the South China Sea. *Journal of Oceanography*
18 62(4):559–575, DOI 10.1007/s10872-006-0076-0

19 Chen HT, Yan XH, Shaw PT, Zheng Q (1996) A numerical simulation of
20 wind stress and topographic effects on the Kuroshio current path near
21 Taiwan. *Journal of physical oceanography* 26(9):1769–1802, DOI 10.1175/
22 1520-0485(1996)026<1769:ANSOWS>2.0.CO;2

- 1 Cruzado A, Velasquez Z (1990) Nutrients and phytoplankton in the Gulf of Li-
2 ons, northwestern Mediterranean. *Continental Shelf Research* 10(911):931–
3 942, DOI 10.1016/0278-4343(90)90068-W
- 4 Csanady GT (1982) *Circulation in the coastal ocean*. Springer
- 5 Dee DP, Uppala SM, Simmons AJ, Berrisford P, Poli P, Kobayashi S, An-
6 drae U, Balmaseda MA, Balsamo G, Bauer P, Bechtold P, Beljaars ACM,
7 van de Berg L, Bidlot J, Bormann N, Delsol C, Dragani R, Fuentes M, Geer
8 AJ, Haimberger L, Healy SB, Hersbach H, Hlm EV, Isaksen L, Kllberg P,
9 Khler M, Matricardi M, McNally AP, Monge-Sanz BM, Morcrette JJ, Park
10 BK, Peubey C, de Rosnay P, Tavolato C, Thépaut JN, Vitart F (2011)
11 The ERA-Interim reanalysis: configuration and performance of the data as-
12 similation system. *Quarterly Journal of the Royal Meteorological Society*
13 137(656):553–597, DOI 10.1002/qj.828
- 14 Deshayes J, Curry R, Msadek R (2014) CMIP5 Model Intercomparison of
15 Freshwater Budget and Circulation in the North Atlantic. *Journal of Cli-
16 mate* 27(9):3298–3317, DOI 10.1175/JCLI-D-12-00700.1
- 17 Echevin V, Crepon M, Mortier L (2003) Interaction of a coastal current with
18 a gulf: Application to the shelf circulation of the Gulf of Lions in the
19 Mediterranean Sea. *Journal of Physical Oceanography* 33(1):188–206, DOI
20 {10.1175/1520-0485(2003)033<0188:IOACCW>2.0.CO;2}
- 21 Estournel C, Broche P, Marsaleix P, Devenon JL, Auclair F, Vehil R (2001)
22 The Rhone River Plume in Unsteady Conditions: Numerical and Exper-
23 imental Results. *Estuarine, Coastal and Shelf Science* 53(1):25–38, DOI

1 10.1006/ecss.2000.0685

2 Fischer C, Montmerle T, Berre L, Auger L, Stefanescu SE (2005) An overview
3 of the variational assimilation in the ALADIN/France numerical weather-
4 prediction system. Quarterly Journal of the Royal Meteorological Society
5 131(613):3477–3492, DOI 10.1256/qj.05.115

6 Fraysse M, Pairaud I, Ross ON, Faure VM, Pinazo C (2014) Intrusion of
7 Rhone River diluted water into the Bay of Marseille: Generation processes
8 and impacts on ecosystem functioning. Journal of Geophysical Research-
9 Oceans 119(10):6535–6556, DOI 10.1002/2014JC010022

10 Gan J, Allen JS (2002) A modeling study of shelf circulation off northern Cal-
11 ifornia in the region of the Coastal Ocean Dynamics Experiment: Response
12 to relaxation of upwelling winds. Journal of Geophysical Research-Oceans
13 107(C9):6–1–6–31, DOI 10.1029/2000JC000768

14 Gatti J (2008) Intrusions du Courant Nord Méditerranéen sur la partie est du
15 plateau continental du Golfe du Lion. PhD thesis, Université Aix-Marseille

16 Gatti J, Petrenko A, Leredde Y, Devenon J (2006) Modelling the intrusions
17 of the northern current on the eastern part of the gulf of lions continental
18 shelf. In: Geophysical Research Abstracts, vol 8, p 00684

19 Gawarkiewicz G, Church TM, Luther GW, Ferdelman TG, Caruso M (1992)
20 Large-scale penetration of Gulf Stream water onto the Continental Shelf
21 north of Cape Hatteras. Geophysical Research Letters 19(4):373–376, DOI
22 10.1029/92GL00225

- 1 Guihou K, Marmain J, Ourmières Y, Molcard A, Zakardjian B, Forget P (2013)
2 A case study of the mesoscale dynamics in the North-Western Mediterranean
3 Sea: a combined datamodel approach. *Ocean Dynamics* 63(7):793–808, DOI
4 10.1007/s10236-013-0619-z
- 5 Huthnance JM (1995) Circulation, exchange and water masses at the ocean
6 margin: the role of physical processes at the shelf edge. *Progress in Oceanog-*
7 *raphy* 35(4):353–431, DOI 10.1016/0079-6611(95)80003-C
- 8 Korotaev G, Oguz T, Nikiforov A, Koblinsky C (2003) Seasonal, interannual,
9 and mesoscale variability of the Black Sea upper layer circulation derived
10 from altimeter data. *Journal of Geophysical Research-Oceans* 108(C4), DOI
11 10.1029/2002JC001508
- 12 Largier JL (2003) Considerations in Estimating Larval Dispersal Distances
13 from Oceanographic Data. *Ecological Applications* 13(1):71–89, DOI 10.
14 1890/1051-0761(2003)013[0071:CIELDD]2.0.CO;2
- 15 Lentz SJ (2001) The Influence of Stratification on the Wind-Driven Cross-Shelf
16 Circulation over the North Carolina Shelf. *Journal of Physical Oceanography*
17 31(9):2749–2760, DOI 10.1175/1520-0485(2001)031<2749:TIOSOT>2.0.CO;
18 2
- 19 Liu KK, Atkinson L, Chen CTA, Gao S, Hall J, MacDonald RW, McManus LT,
20 Quiones R (2000) Exploring continental margin carbon fluxes on a global
21 scale. *Eos, Transactions American Geophysical Union* 81(52):641–644, DOI
22 10.1029/EO081i052p00641-01

-
- 1 Madec G (2008) NEMO ocean engine. Tech. rep., Institut Pierre-Simon
2 Laplace
- 3 Mantoura RFC, Martin JM, Wollast R, et al (1991) Ocean margin processes
4 in global change. John Wiley and Sons Ltd.
- 5 Millot C (1979) Wind induced upwellings in the Gulf of Lions. *Oceanologica*
6 *Acta* 2(3):261–274
- 7 Millot C (1990) The Gulf of Lions’ hydrodynamics. *Continental Shelf Research*
8 10(911):885–894, DOI 10.1016/0278-4343(90)90065-T
- 9 Millot C (1999) Circulation in the Western Mediterranean Sea. *Journal of*
10 *Marine Systems* 20(1-4):423–442, DOI 10.1016/S0924-7963(98)00078-5
- 11 Millot C, Wald L (1980) The effect of Mistral wind on the Ligurian current
12 near Provence. *Oceanologica Acta* 3(4):399–402
- 13 Oey LY, Atkinson LP, Blanton JO (1987) Shoreward intrusion of upper
14 Gulf Stream water onto the US southeastern continental shelf. *Journal*
15 *of physical oceanography* 17(12):2318–2333, DOI 10.1175/1520-0485(1987)
16 017<2318:SIOUGS>2.0.CO;2
- 17 Oguz T, Besiktepe S (1999) Observations on the Rim Current structure,
18 CIW formation and transport in the western Black Sea. *Deep Sea Re-*
19 *search Part I: Oceanographic Research Papers* 46(10):1733–1753, DOI
20 10.1016/S0967-0637(99)00028-X
- 21 Ourmières Y, Zakardjian B, Beranger K, Langlais C (2011) Assessment of a
22 NEMO-based downscaling experiment for the North-Western Mediterranean
23 region: Impacts on the Northern Current and comparison with ADCP data

- 1 and altimetry products. *Ocean Modelling* 39(3-4):386–404, DOI 10.1016/j.
2 ocemod.2011.06.002
- 3 Petrenko A (2003) Variability of circulation features in the gulf of lion NW
4 Mediterranean Sea. Importance of inertial currents. *Oceanologica Acta*
5 26(4):323–338, DOI 10.1016/S0399-1784(03)00038-0
- 6 Ponte RM (2006) Low-frequency sea level variability and the inverted barom-
7 eter effect. *Journal of Atmospheric and Oceanic Technology* 23(4):619–629,
8 DOI 10.1175/JTECH1864.1
- 9 Reffray G, Fraunié P, Marsaleix P (2004) Secondary flows induced by wind
10 forcing in the Rhône region of freshwater influence. *Ocean Dynamics*
11 54(2):179–196, DOI 10.1007/s10236-003-0079-y
- 12 Ross O, Fraysse M, Pinazo C, Pairaud I () Impact of an intrusion by the
13 Northern Current on the biogeochemistry in the eastern Gulf of Lion, NW
14 Mediterranean. *Estuarine, Coastal and Shelf Science*
- 15 Schaeffer A, Garreau P, Molcard A, Fraunie P, Seity Y (2011) Influence of
16 high-resolution wind forcing on hydrodynamic modeling of the Gulf of Lions.
17 *Ocean Dynamics* 61(11):1823–1844, DOI 10.1007/s10236-011-0442-3
- 18 Tang T, Hsueh Y, Yang Y, Ma J (1999) Continental slope flow northeast of
19 Taiwan. *Journal of Physical Oceanography* 29(6):1353–1362, DOI 10.1175/
20 1520-0485(1999)029<1353:CSFNOT>2.0.CO;2
- 21 Ulses C, Estournel C, Puig P, Durrieu de Madron X, Marsaleix P (2008)
22 Dense shelf water cascading in the northwestern mediterranean during the
23 cold winter 2005: Quantification of the export through the gulf of lion and

-
- 1 the catalan margin. *Geophysical Research Letters* 35(7):1–6, DOI 10.1029/
2 2008GL033257, URL <http://dx.doi.org/10.1029/2008GL033257>, 107610
- 3 Wolanski E, Norro A, King B (1995) Water circulation in the Gulf of Papua.
4 *Continental Shelf Research* 15(2):185–212, DOI 10.1016/0278-4343(94)
5 E0026-I
- 6 Wu CR, Tang T, Lin S (2005) Intra-seasonal variation in the velocity field of
7 the northeastern South China Sea. *Continental Shelf Research* 25(17):2075–
8 2083, DOI 10.1016/j.csr.2005.03.005